Biochimica et Biophysica Acta, 1150 (1993) 155–161
© 1993 Elsevier Science Publishers B.V. All rights reserved 0005-2736/93/$06.00

BBAMEM 76042

Accessibility of spin-labeled phospholipids in anionic and zwitterionic bilayer membranes to paramagnetic relaxation agents. Continuous wave power saturation EPR studies

Margot M.E. Snel and Derek Marsh

Max-Planck-Institut für biophysikalische Chemie, Abteilung für Spektroskopie, Göttingen (Germany)

(Received 16 February 1993)

Key words: EPR; Spin label; Phosphatidylglycerol; Lipid bilayer; Phospholipid

The location of phospholipids, spin-labeled in the headgroup or at various positions of the *sn*-2 chain, incorporated in bilayer membranes of dimyristoylphosphatidylcholine, dimyristoylphosphatidylglycerol or dioleoylphosphatidylglycerol, has been calibrated in terms of their accessibility to paramagnetic relaxation agents. A power saturation approach has been used to determine the spin-label relaxation times, which in turn is influenced by spin–spin interactions with the different paramagnetic species. The effect of different paramagnetic relaxation agents on the power saturation behaviour of the spin-labeled lipids has been used to determine the relaxation enhancement which is quantified in terms of an accessibility parameter. Molecular oxygen, which dissolves preferentially in the lipid phase and the water-soluble, membrane-impermeant chromium oxalate anion are shown to report reliably on the accessibility of spin-labels located in one of the two phases. On the other hand, an uncharged, polar nickel-iminodiacetic acid complex is shown to enhance relaxation of spin-labels in both phases. These calibrations are essential for the study of the interaction of basic proteins with anionic lipid membranes.

Introduction

The spin-label EPR technique is capable of yielding structural and dynamic information on lipids and proteins, the components that constitute biological membranes. Spin-labeling in combination with spin-probes (chemically inert paramagnetic species) is an effective tool for studying the localization of spin-labels at the membrane surface or within membranes [1]. Recently, Hubbell and coworkers have used the method to investigate the membrane topography of specifically spin-labeled bacteriorhodopsin, melittin and colicin E1 [2–4]. Other potential applications include studies of the interaction of peripheral and membrane-penetrant proteins, such as cytochrome *c* and apocytochrome *c*, respectively, with negatively charged lipid membranes. The method is based on the exposure of the nitroxide spin-labels to paramagnetic relaxation agents, that are soluble either in the lipid phase or in the aqueous phase. The effect of the paramagnetic species can be monitored either by pulse saturation recovery or by continuous wave (CW) power saturation EPR spectroscopy of the spin-labeled species. Changes in the nitroxide relaxation times due to interactions with the fast-relaxing paramagnetic species are a measure of their accessibility to the nitroxide group.

Molecular oxygen and chromium oxalate are well-known examples of paramagnetic agents that preferentially dissolve, respectively, in the membrane interior [5–7] and in the aqueous phase [8,9]. However a potential disadvantage of the use of chromium oxalate, particularly with membranes containing anionic lipids, is its negative charge. By using an uncharged, polar relaxation agent as probe for the aqueous phase, in principle, this problem should be overcome. In this study the nickel-iminodiacetic acid complex, is tested for this purpose.

Correspondence to: D. Marsh, Max-Planck-Institut für biophysikalische Chemie, Abteilung für Spektroskopie, Postfach 2841, 37018 Göttingen, Germany.

Abbreviations: EPR, electron spin resonance; CW, continuous wave; DMPC, 1,2-dimyristoyl-*sn*-glycero-3-phosphocholine; DMPG, 1,2-dimyristoyl-*sn*-glycero-3-phosphoglycerol; DOPG, 1,2-dioleoyl-*sn*-glycero-3-phosphoglycerol; Tempo-stearamide, 4-(octadecanoyl)amino-2,2,6,6-tetramethylpiperidine-1-oxyl; *n*-PCSL, 1-acyl-2-[*n*-(4,4-dimethyloxazolidine-*N* -oxyl)]stearoyl-*sn*-glycero-3- phosphocholine; *n*-PGSL, 1-acyl-2-[*n*-(4,4-dimethyloxazolidine-*N*-oxyl)]stearoyl-*sn*-glycero-3-phosphoglycerol; T-PASL, 4-phosphatidyl-2,2,6,6-tetramethylpiperidine-1-oxyl; Ni-IDA, nickel-iminodiacetic acid; Hepes, *N*-(2-hydroxyethyl) piperazine-*N'*-2-ethanesulfonic acid; CROX, potassium tris(oxalato)chromate(III) trihydrate.

A complication in the application of the CW saturation method is the need to take into account the inhomogeneous broadening that is almost invariably present in the EPR spectra from spin-labels in biological systems (cf. Ref. 10). Recently, methods have been introduced that allow quite generally for inhomogeneous broadening in the analysis of the saturation curves [11], that are obtained in a CW progressive power saturation EPR experiment. This analysis uses the total spectral intensity instead of the first derivative EPR signal amplitude to describe the saturation behaviour and yields effective values for the product of the spin-lattice (T_1) and the spin-spin (T_2) relaxation times of the nitroxide spin-label. Paramagnetic species, that have short spin-lattice relaxation times are able to decrease the relaxation times of the nitroxide spin-labels by spin–spin interactions [1]. The efficiency of this process depends on the concentration and the diffusion constant of the paramagnetic species [3,12]. The difference in the rate of the nitroxide relaxation in the presence and in the absence of paramagnetic species provides a measure for the accessibility of the nitroxide spin-label to the paramagnetic relaxing molecule, and is used as an accessibility parameter.

In this study the accessibility of phospholipids spin-labeled in the headgroup and at various positions in the *sn*-2 chain to the relaxation agents oxygen, chromium oxalate and nickel-iminodiacetic acid is determined. The phospholipid bilayer membranes that are examined, are composed of dimyristoylphosphatidylcholine (DMPC), dimyristoylphosphatidylglycerol (DMPG) and dioleoylphosphatidylglycerol (DOPG). The use of negatively charged membranes is particularly important, because calibration of the accessibility of the paramagnetic agents is essential for the study of the interaction with basic, peripheral and membrane-penetrating proteins.

Materials and Methods

Materials

DMPG was synthesized from DMPC (Fluka, Buchs, Switzerland) by a headgroup exchange reaction catalyzed by phospholipase D [13]. DOPG was obtained from Avanti (Birmingham, AL). 4-(Octadecanoyl)amino-2,2,6,6-tetramethylpiperidine-1-oxyl (Tempostearamide) was obtained from Molecular Probes (Roseville, MN). Phosphatidylglycerols (*n*-PGSL) and phosphatidylcholines (*n*-PCSL) spin-labeled at different positions in the *sn*-2 chain, were synthesized by B. Angerstein, essentially as described in Ref. 14. 4-Phosphatidyl-2,2,6,6-tetramethyl-piperidine-1-oxyl (T-PASL) was prepared by H. Eibl and A. Watts at this Institute by phosphorylating 4-hydroxy-2,2,6,6-tetramethylpiperidine-1-oxyl with $POCl_3$ and condensing with 1,2-dipalmitoyl-*sn*-glycerol, essentially according to the method of Eibl [15]. Spin-labeled apocytochrome *c* was prepared by aqueous reaction with spin-labeled maleimide (Aldrich, Milwaukee, WI) as will be described in detail elsewhere. A 0.25 M stock solution of nickel/iminodiacetic acid (Ni-IDA) was prepared by adding 1 volume of a 1.5 M nickel(II) chloride solution containing 60 mM Hepes to 5 volumes of an aqueous 0.3 M iminodiacetic acid solution. The logarithm of the stability constant of the complex is 8.3 [16]. Potassium tris(oxalato)chromate(III) trihydrate (CROX) was synthesized essentially as described by Bailar and Jones [17] and characterized by its absorption spectrum [18,19].

EPR sample preparation

All experiments were performed in a buffer containing 10 mM Hepes, 50 mM NaCl (pH 7.0). For experiments in the presence or in the absence of oxygen this buffer was saturated either with oxygen or argon, respectively. The Ni-IDA stock solution was diluted to 1 or 2 mM with argonated-buffer and CROX was dissolved freshly at 50 mM or 5 mM in argonated-buffer.

Lipid films were prepared by dissolving 1 mg DMPG, DMPC or 0.5 mg DOPG with 1 mol% of spin-label in chloroform/methanol (2:1, v/v). Additionally, the DOPG solutions contained 0.1 mol% butylated hydroxytoluene to prevent lipid peroxidation. The solution was evaporated with a stream of nitrogen and the residual traces of solvent were removed under vacuum. The required buffer was added to the dry lipid: 200 μl of either oxygenated-, argonated- or 50 mM CROX-containing buffer for the respective DMPC samples; 200 μl 1 mM Ni-IDA buffer for DMPG samples in the presence of Ni-IDA; 50 μl and 25 μl of oxygenated- or argonated-buffer for DMPG and DOPG samples in the presence and in the absence of oxygen, respectively. After flushing the tubes with oxygen or argon, as required, the lipid was hydrated by warming above the gel-to-fluid phase transition and vortexing. After 5 cycles of freezing and thawing, the samples were incubated at 37°C for 30 min. The DMPC dispersions were centrifuged in a Labofuge II (Heraeus, $1000 \times g$, 15 min) and the DMPG/Ni-IDA dispersions in a Biofuge A (Heraeus, $15000 \times g$, 20 min), after which the concentrated lipid dispersions were transferred with 30 μl of the appropriate buffer to EPR capillaries that were flushed with oxygen or argon. The EPR samples were concentrated further by centrifugation (DMPC: Labofuge II, $1000 \times g$, 10 min; DMPG: Biofuge A, $10000 \times g$, 10 min). Excess supernatant and lipid were removed to obtain samples ≤ 5 mm in length to avoid inhomogeneities of the microwave and modulation fields in the EPR cavity. The capillaries were sealed after flushing with either oxygen or argon.

For the DMPG and DOPG dispersions with or without oxygen present, the samples after incubation

were transferred directly to EPR capillaries that were flushed either with oxygen or argon. The EPR samples were then prepared further as described above for DMPC dispersions.

For preparation of spin-labeled apocytochrome *c* samples, protein solutions at a concentration of 160 μM were flushed with oxygen or argon and transferred to EPR capillaries which were also flushed with oxygen or argon (sample length ≤ 5 mm). Protein solutions containing 1 mM CROX or Ni-IDA were prepared by diluting the argonated solution of spin-labeled apocytochrome *c* with 5 mM CROX buffer (4:1, v/v) or with 2 mM Ni-IDA buffer (1:1, v/v).

EPR spectroscopy

EPR measurements were performed on a Varian E-12 Century Line 9 GHz EPR spectrometer. Sample capillaries were centered in a standard 4 mm quartz tube containing light silicone oil for thermal stability; temperature was regulated with a nitrogen gas flow system. Conventional, in phase, absorption spectra were recorded with a modulation frequency of 100 kHz and a modulation amplitude of 1.25 Gauss p–p at various microwave powers decreasing from 180 mW to 0.03 mW. This corresponds to an root-mean-square (r.m.s.) microwave magnetic field, $\langle H_1^2 \rangle^{1/2}$, at the sample ranging from approx. 600 to 6 mGauss. A standardized sample configuration was used in all CW saturation experiments [20,21] and all measurements were performed under critical coupling conditions. The microwave field was calibrated by measuring the CW saturation properties of deoxygenated aqueous peroxylamine disulphonate, as described by Kooser et al. [22]. The microwave cavity Q was measured as described in [20] and corresponding corrections made in calculating the r.m.s. microwave field, $\langle H_1^2 \rangle^{1/2}$ at the sample. The total static field scan width was 100 Gauss.

Analysis of saturation curves

To obtain a saturation curve, the spectral intensity (second integral of the first derivative spin-label EPR spectrum) was determined as a function of the microwave magnetic field, H_1, at the sample. The saturation of the integrated spectral intensity is described by [11,23]:

$$\text{Intensity} = A_o H_1 / \left(1 + \gamma^2 H_1^2 T_1 T_2\right)^{1/2} \qquad (1)$$

where A_o is a normalization factor, γ is the gyromagnetic ratio of the electron, and T_1 and T_2 are the spin-lattice and spin-spin relaxation times, respectively, of the spin-label. The experimental data were fit to this equation using a nonlinear least-squares method with the effective T_1T_2 product and the normalization factor as the adjustable parameters. In the presence of a fast-relaxing paramagnetic species, the spin-lattice relaxation rate, $1/T_1$, of the spin-label will be enhanced by an amount which is linearly proportional to the concentration, *c*, of the fast-relaxing species:

$$1/T_1 = 1/T_1^o + k_{RL}c \qquad (2)$$

where T_1^o is the value of T_1 for $c = 0$, and k_{RL} is a constant which depends on the diffusion coefficient and cross-section for collision of the fast-relaxing species in the case of the Heisenberg spin exchange interaction and the distance of closest approach to the spin-label in the case of the magnetic dipole–dipole interaction (see e.g. Ref. 24). For the particular case of collisions with molecular oxygen, $k_{RL} = 4\pi r_o D_{O_2}$ where r_o is the interaction distance between oxygen and the spin-label (approx. 4.5 Å) and D_{O_2} is the diffusion coefficient of oxygen [7]. Thus k_{RL} is a measure of the accessibility of the paramagnetic relaxation agent to the spin-label. In principle, the presence of the paramagnetic species will also lead to an increase in the T_2 relaxation rate, but for the systems of interest and at the concentrations of relaxation agent used the effects on the spin-lattice relaxation (T_1) will dominate. Additionally, $T_2 \ll T_1$ thus the T_2 relaxation rate remains essentially constant at the value T_2^o obtained in the absence of paramagnetic relaxation agents. The dependence of the T_1T_2 product obtained from the CW saturation studies on the concentration of paramagnetic relaxation agent is therefore given by:

$$1/T_1T_2 = 1/(T_1T_2)^o + (k_{RL}/T_2^o)c \qquad (3)$$

This means that the accessibility, (k_{RL}/T_2^o), only can be compared directly for nitroxides with a similar T_2, i.e., for samples with a similar linewidth. To enable comparison between spin-label samples with different linewidths the accessibility is normalized with respect to the linewidth ($\delta \propto 1/T_2^o$) which corresponds to the peak-to-peak width of the central line ($m_I = 0$) in the EPR spectrum under non-saturating conditions and in the absence of paramagnetic relaxation agents. Thus an accessibility parameter can be defined as the difference in the reciprocal T_1T_2 product for the nitroxide group in the presence (p) and in the absence (o) of the paramagnetic species, divided by the linewidth (δ) of the $m_I = 0$ line:

$$\text{Acc. par.} = \left[(1/T_1T_2)_p - (1/T_1T_2)_o\right] / \delta \ (\cdot 10^{13}\ \text{s}^{-2}\,\text{Gauss}^{-1}) \qquad (4)$$

Results and Discussion

CW saturation behaviour

The dependences on microwave power of the EPR spectra of the 5-PGSL spin-label in liquid-crystalline

DOPG dispersions in the presence and in the absence of oxygen that were obtained in CW power saturation EPR experiments are given in Fig. 1. At a given microwave power, the spectra are normalized to the same spin concentration and therefore reflect the differences in spectral amplitude resulting from the differential saturation of the overall spectral intensity as well as from the different degrees of saturation broadening of the spectral lineshape in the presence and absence of oxygen. The saturation broadening with increasing microwave power is clearly visible in the spectra of the sample in the absence of oxygen, whereas it is nearly absent in the spectra of the sample with oxygen present. Thus, although the EPR spectra consist of anisotropic powder patterns, i.e., are inhomogeneously broadened, the additional homogeneous broadening occurring at higher microwave powers must be taken into account in the analysis of the power saturation curves. This is done by evaluating the saturation behaviour of the double integrated intensity of the entire spectrum, since this quantity is not sensitive to saturation broadening, i.e., is independent of the degree of inhomogeneous spectral broadening [11]. Unlike for the spectral line heights, the saturation of the integrated spectral intensity therefore can vary throughout the spectrum only because of the anisotropy in the T_1 and T_2 relaxation times, and not because of the saturation broadening. Also, for the cases considered here, the anisotropy of T_2 remains constant because, at the concentrations used, the paramagnetic relaxation reagents do not cause appreciable spectral broadening.

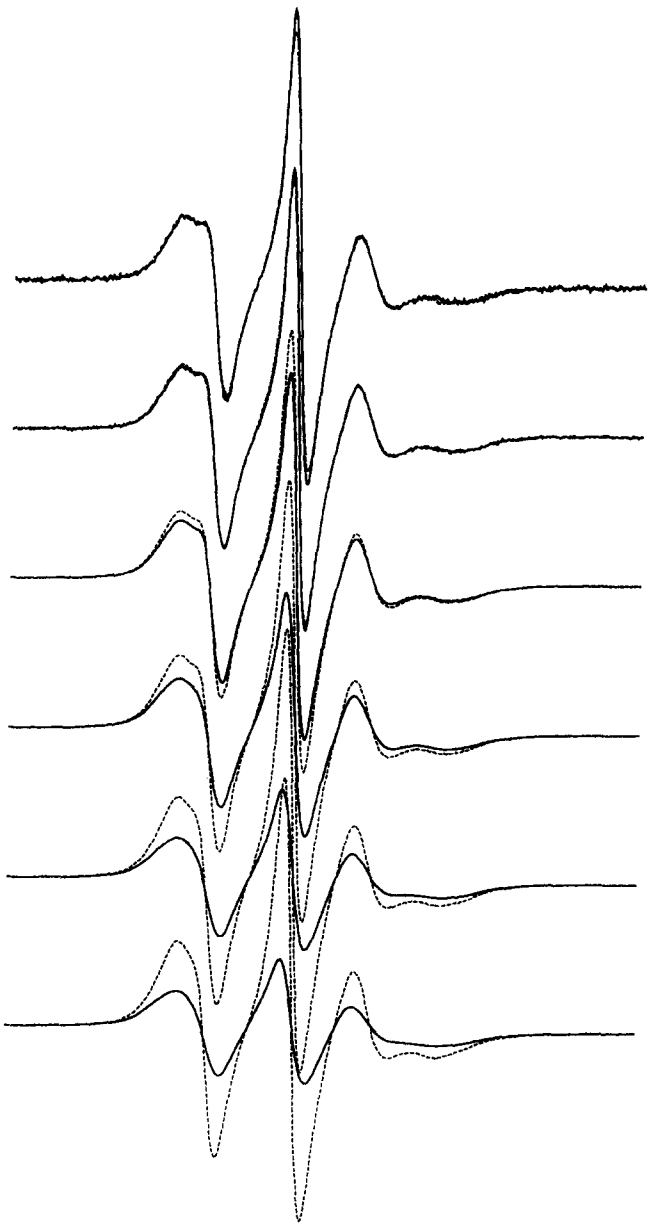

Fig. 1. EPR spectra of the 5-PGSL spin-label in DOPG dispersions in the absence (solid lines) and in the presence (dashed lines) of oxygen recorded at different root-mean-square microwave magnetic fields, $\langle H_1^2 \rangle^{1/2}$, at the sample. From top to bottom, the microwave power at which the spectra are recorded is increasing: corresponding to $\langle H_1^2 \rangle^{1/2} = 19$, 58, 172, 300, 418 and 522 mGauss. Temperature is 30°C. Total scan width is 100 Gauss. The spectra within each pair are normalized to the same spin concentration.

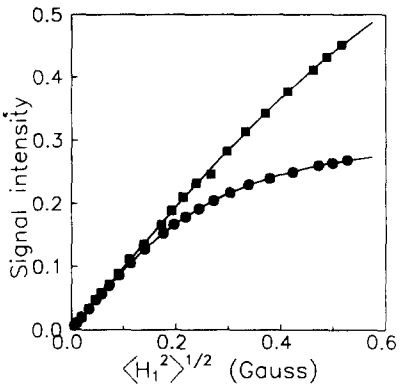

Fig. 2. Dependence of the double-integrated intensity of the EPR spectrum recorded at 30°C of the 5-PGSL phosphatidylglycerol spin-label in aqueous bilayer dispersions of DOPG in the presence (■) and in the absence (●) of oxygen on the root-mean-square microwave magnetic field, $\langle H_1^2 \rangle^{1/2}$, at the sample. The signal intensities are normalized relative to the number of spin-labels in each sample, corresponding to $A_0 = 1$ in Eqn. 1. The solid lines show the results of the nonlinear least-squares fits of the saturation curves according to Eqn. 1, yielding $T_1T_2 = 3.3 \cdot 10^{-14}$ s^2 in the absence and $T_1T_2 = 3.8 \cdot 10^{-15}$ s^2 in the presence of oxygen.

The saturation curves for the double-integrated intensity of the spectra given in Fig. 1 are depicted in Fig. 2. The effect of the paramagnetic relaxation enhancement is clear: oxygen reduces the degree of saturation of the spin-label at any given microwave power beyond the initial linear region. The saturation curves were fitted to Eqn. 1 yielding values of $T_1T_2 = 3.3 \cdot 10^{-14}$ s^2 in the absence of oxygen and $T_1T_2 = 3.8 \cdot 10^{-15}$ s^2 in the presence of oxygen. The high quality of the fits given in Fig. 2, demonstrates that the method of analysis based on Eqn. 1 for the saturation of the

integrated intensity of the EPR spectrum successfully handles the problem of inhomogeneous broadening, since, as noted above, the spectrum of the 5-PGSL spin-label in this system consists of an anisotropic powder pattern with unresolved proton hyperfine structure (Fig. 1). Also, it is seen from the fits that any effects of anisotropy in T_1 and T_2 are handled in a reasonably adequate manner by taking an effective average value in the integration over the entire spectrum (cf. Ref. 11). The difference in the reciprocal of the T_1T_2 products divided by the linewidth of the central line has been defined above as the accessibility parameter, which in this case amounts to $8.0 \cdot 10^{13}$ s^{-2} Gauss^{-1}. The accessibility parameters of the different paramagnetic species to various spin-labeled lipids in zwitterionic and anionic lipid bilayer membranes are summarized in Figs. 3 and 4, respectively, that are given below.

Accessibility profiles in phosphatidylcholine bilayers

In order to determine the accessibility of the various paramagnetic relaxation agents to nitroxide free radicals positioned at different locations within the membrane, at the membrane surface and external to the membrane, the power saturation behaviour of the EPR spectra of a range of spin-labeled species has been studied. Phosphatidylcholines and phosphatidylglycerols spin-labeled at different C-atoms in the hydrocarbon chain (*n*-PCSL and *n*-PGSL), phosphatidic acid labeled at the phosphate of the lipid headgroup (T-PASL), a stearamide spin-label for which the nitroxide group will be positioned at the membrane surface (Tempo-stearamide), and spin-labeled apocytochrome *c* in aqueous solution were used for this purpose. Spatial discrimination is achieved by the preferential partitioning of the relaxation agents between the aqueous and membrane phases.

The profile, with position of the spin-label in the membrane, of the accessibility parameters to oxygen and chromium oxalate in dispersions of the zwitterionic DMPC in the fluid phase are shown in Fig. 3. For comparison, the accessibility parameters for spin-labeled apocytochrome *c* in the aqueous phase to the same relaxation agents are also given. The oxygen accessibility is relatively low in the aqueous phase and in the phospholipid headgroup region but increases towards the centre of the membrane. This is consistent with the known preference of oxygen to dissolve in the hydrocarbon phase and in good agreement with the oxygen transport parameters in DMPC at 29°C obtained for stearic acid spin-labels by long-pulse saturation recovery EPR techniques [25].

Accessibility parameters to the anionic chromium oxalate (50 mM) for the negatively charged headgroup spin-label, T-PASL, incorporated in DMPC bilayers and in mixed bilayers consisting of DMPG/DMPC

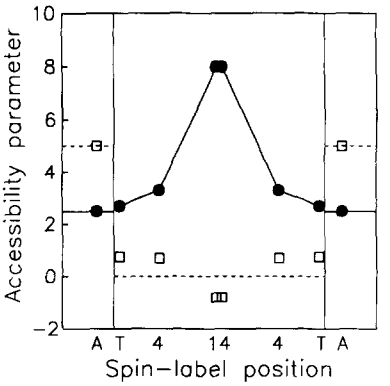

Fig. 3. Dependence on location of the spin-label group in DMPC bilayers of the accessibility to oxygen (●, solid line) and to chromium oxalate (□, dashed line). The accessibility parameter (in units of 10^{13} s^{-2} Gauss^{-1}) for uncharged (T: Tempo-stearamide) and zwitterionic spin-labeled lipids (4, 14: *n*-PCSL) and of spin-labeled apocytochrome *c* (A) in solution is plotted as the membrane profile of the position of the spin-label group. The vertical lines indicating the surface of the membrane have a separation of ~ 40 Å. The chromium oxalate concentration in the protein solution is 1 mM and in the lipid dispersions is 50 mM, and both solutions are argonated. For experiments in the presence of molecular oxygen, the solutions are saturated with pure oxygen. Temperature of the measurements is 30°C.

(15:85, mol/mol) in 50 mM NaCl or 1 M NaCl buffer were measured (data not shown). No significant effect on the saturation behaviour of the T-PASL spin-label in these lipid bilayers could be observed, which might be explained by the negative charge on the spin-label, although at high salt concentrations electrostatic effects are expected to be minimal. Therefore the accessibility profile of chromium oxalate was determined with uncharged and zwitterionic spin-labels in zwitterionic DMPC bilayer membranes. Compared to oxygen, the accessibility parameter to chromium oxalate shows qualitatively the inverse profile with position of the spin-label in the membrane. Spin-labels located in the phospholipid headgroup region as well as in the membrane interior are not significantly affected in their saturation behaviour even by 50 mM chromium oxalate, whereas the spin-label on apocytochrome *c* in the aqueous phase has a high accessibility to 1 mM chromium oxalate. Because there is no net negative charge in these zwitterionic DMPC dispersions the inaccessibility of the spin-labels located at the membrane surface and in the membrane interior is due mainly to the impermeability of the negatively charged chromium oxalate. This is in agreement with the inaccessibility of a membrane-buried androstane spin-label to chromium oxalate found by Altenbach et al. [3].

Accessibility profiles in phosphatidylglycerol bilayers

The oxygen accessibility parameters for negatively charged spin-labeled phospholipids incorporated into negatively charged DMPG and DOPG bilayers at a temperature in the fluid phase are shown in Fig. 4. The

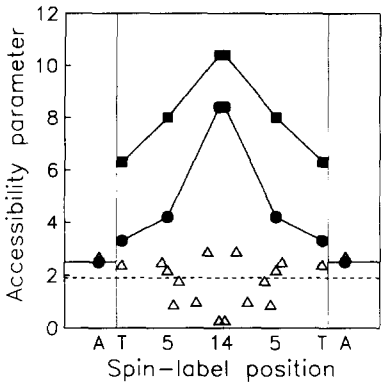

Fig. 4. Dependence on location of the spin-label group in DMPG (●, △) and in DOPG (■) bilayers of the accessibility to oxygen (solid lines) and to Ni-IDA (dashed line). The accessibility parameter (in units of 10^{13} s^{-2} $Gauss^{-1}$) for negatively charged spin-labeled lipids (5, 14: *n*-PGSL and T: Tempo-PASL) and of spin-labeled apocytochrome *c* (A) in solution is plotted as the membrane profile of the position of the spin-label group. The vertical lines indicating the surface of the membrane have a separation of ~ 40 Å. The Ni-IDA concentration in the samples is 1 mM and they are argonated. For experiments in the presence of molecular oxygen the solutions are saturated with pure oxygen. Temperature of the measurements is 30°C.

oxygen accessibility parameters in the DMPG model membranes are rather similar to those obtained for the zwitterionic spin-labels in DMPC membranes. The oxygen accessibility parameters for the spin-labeled lipids in the same DMPG system at 10°C, when the lipid is in the gel phase, were low in the region of $0.4 \cdot 10^{13}$ s^{-2} $Gauss^{-1}$ (data not shown) and showed a flat membrane profile, qualitatively comparable to that measured by Subczynski et al. [25] with spin-labeled fatty acids in a DMPC system. The oxygen accessibility of the spin-labels in DOPG dispersions is significantly higher than that in DMPG. This might be explained by a different oxygen concentration and/or diffusion constant in the different membranes, even though at 30°C both lipids are in the liquid-crystalline phase. DOPG dispersions which have a gel-to-fluid phase transition temperature at $T_t = -20$°C are probably more fluid than those of DMPG whose phase transition is at $T_t = 23$°C, which could explain the enhanced oxygen concentration and diffusion constant in the DOPG membranes. This explanation is supported by comparison with the results obtained for DMPG in the gel phase. The more similar oxygen accessibility parameters that are observed in the centre of the bilayer for phosphatidylglycerols with saturated and unsaturated chains could be due to a locally higher fluidity in this region of the membrane and to the higher mobility of spin-labels attached closer to the terminal methyl group of the acyl chains, hence reflecting the characteristic flexibility gradient in fluid lipid bilayers [26].

The accessibility parameters to the neutral Ni-IDA complex for negatively charged spin-labeled phospholipids in DMPG membranes and spin-labeled apocytochrome *c* in the aqueous phase are also shown in Fig. 4. In contrast to the results obtained with oxygen and chromium oxalate, the accessibility parameters to Ni-IDA are similar for spin-labels located both in the aqueous phase and in the hydrophobic region of the membrane. This demonstrates clearly that the electroneutral Ni-IDA complex partitions between the aqueous and membrane phases. At higher concentrations (5 mM) of Ni-IDA the outer hyperfine splitting (i.e., the distance between high- and low-field extrema) of the 5-PGSL spin-label is increased by 2 Gauss (data not shown), indicating that the mobility of the spin-label is decreased by partitioning of Ni-IDA into the membrane. Both the decreased spin-label mobility and the nonspecificity of Ni-IDA are strong indications that the Ni-IDA complex accumulates in the membrane, which makes it less suitable as a paramagnetic relaxation agent for discriminating between the aqueous and the lipid phases. It has been suggested [12] that the neutral relaxation agent cobalt acetylacetonate is located preferentially at the polar/apolar interface of lipid membranes, but the present results on the relaxation enhancement by Ni-IDA of phosphatidylglycerols labeled at many different positions in the lipid chain (Fig. 4), indicate that this might not be the case.

Conclusions

In summary, the method used to analyse the saturation curves obtained by continuous wave power saturation EPR spectroscopy and the accessibility parameters derived have been shown to be applicable also to determination of the spin-label location in anionic lipid bilayer systems, thus extending previously published work on zwitterionic lipid systems. Molecular oxygen and chromium oxalate reliably report on the accessibilities of spin-labels located in the lipid phase and in the aqueous phase, respectively. The calibrations established here will be useful for the study of the interaction of spin-labeled peripheral and penetrant proteins with membranes, by the same technique.

References

1 Likhtenshtein, G.I. (1976) Spin Labeling Methods in Molecular Biology (Buchachenko, A.L., ed.), Wiley-Interscience, New York.
2 Altenbach, C., Flitsch, S.L., Khorana, H.G. and Hubbell, W.L. (1989) Biochemistry 28, 7806–7812.
3 Altenbach, C., Froncisz, W., Hyde, J.S. and Hubbell, W.L. (1989) Biophys. J. 56, 1183–1191.
4 Todd, A.P., Cong, J., Levinthal, F., Levinthal, C. and Hubbell, W.L. (1989) Proteins 6, 294–305.
5 Subczynski, W.K. and Hyde, J.S. (1981) Biochim. Biophys. Acta 643, 283–291.
6 Subczynski, W.K. and Hyde, J.S. (1983) Biophys. J. 41, 283–286.
7 Subczynski, W.K. and Hyde, J.S. (1984) Biophys. J. 45, 743–748.
8 Berg, S.P. and Nesbitt, D.M. (1979) Biochim. Biophys. Acta 548, 608–615.

9 Yager, T.D., Eaton, G.R. and Eaton, S.S. (1979) Inorg. Chem. 18, 725–727.
10 Castner, T.G., Jr. (1959) Phys. Rev. 115, 1506–1515.
11 Páli, T., Horváth, L.I. and Marsh, D. (1993) J. Magn. Reson. 101, 215–219.
12 Likhtenshtein, G.I., Kulikov, A.V., Kotelnikov, A.I. and Levchenko, L.A. (1986) J. Biochem. Biophys. Methods 12, 1–28.
13 Comfurius, P. and Zwaal, R.F.A. (1977) Biochim. Biophys. Acta 488, 36–42.
14 Marsh, D. and Watts, A. (1982) Lipid–Protein Interactions, Vol. 2 (Jost, P.C. and Griffith, O.H., eds.), Wiley-Interscience, New York.
15 Eibl, H. (1978) Proc. Natl. Acad. Sci. USA 75, 4074–4077.
16 Chaberek, S., Jr. and Martell, A.E. (1952) J. Am. Chem. Soc. 74, 5052–5056.
17 Bailar, J.C., Jr. and Jones, E.M. (1939) Inorg. Synth. 1, 35–38.
18 Malati, M.A. and Abdul Azim, A.A. (1959) Egypt. J. Chem. 2, 47.
19 Malati, M.A. and Abdul Azim, A.A. (1960) Chem. Abstr. 54, 2085f.
20 Fajer, P. and Marsh, D. (1982) J. Magn. Reson. 49, 212–224.
21 Hemminga, M.A., De Jager, P.A., Marsh, D. and Fajer, P. (1984) J. Magn. Reson. 59, 160–163.
22 Kooser, R.G., Volland, W.V. and Freed, J.H. (1969) J. Chem. Phys. 50, 5243–5257.
23 Portis, A.M. (1953) Phys. Rev. 91, 1071–1078.
24 Marsh, D. (1992) Appl. Magn. Reson. 3, 53–65.
25 Subczynski, W.K., Hyde, J.S. and Kusumi, A. (1989) Proc. Natl. Acad. Sci. USA 86, 4474–4478.
26 Moser, M., Marsh, D., Meier, P., Wassmer, K.-H. and Kothe, G. (1989) Biophys. J. 55, 111–123.